

# Attribution of NAO Predictive Skill beyond Two Weeks in Boreal Winter

Lantao Sun<sup>1</sup>, Judith Perlwitz<sup>2</sup>, Jadwiga H. Richter<sup>3</sup>, Martin P. Hoerling<sup>2</sup>, and James Wilson Hurrell<sup>1</sup>

<sup>1</sup>Colorado State University

<sup>2</sup>National Oceanic and Atmospheric Administration (NOAA)

<sup>3</sup>National Center for Atmospheric Research (UCAR)

November 23, 2022

## Abstract

The week 3-6 averaged winter North Atlantic Oscillation (NAO) predictive skill in a state-of-the-art coupled climate prediction system is attributed to two principle sources: upper and lower boundary conditions linked to the stratosphere and El Niño-Southern Oscillation (ENSO), respectively. A 20-member ensemble of 45-day reforecasts over 1999-2015 is utilized, together with uninitialized simulations with the atmospheric component of the prediction system forced with observed radiative forcing and lower boundary conditions. NAO forecast skill for lead times out to six weeks is higher following extreme stratospheric polar vortex conditions (weak and strong vortex events) compared to neutral states. Enhanced week 3-6 NAO predictive skill for weak vortex events results primarily from stratospheric downward coupling to the troposphere, while enhanced skill for strong vortex events can be partly attributed to lower boundary forcing related to the ENSO phenomenon. Implications for forecast system development and improvement are discussed.

# Attribution of NAO Predictive Skill beyond Two Weeks in Boreal Winter

Lantao Sun<sup>1\*</sup>, Judith Perlwitz<sup>2</sup>, Jadwiga (Yaga) Richter<sup>3</sup>,

Martin Hoerling<sup>2</sup>, James W. Hurrell<sup>1</sup>

<sup>1</sup> Department of Atmospheric Science, Colorado State University, Fort Collins, CO

<sup>2</sup>NOAA Physical Sciences Laboratory, Boulder, CO

<sup>3</sup>National Center for Atmospheric Research, Boulder, CO

Submitted to *Geophysical Research Letters*

Aug 19, 2020

\*Corresponding author: Lantao Sun ([lantao.sun@colostate.edu](mailto:lantao.sun@colostate.edu))

## Key Points:

- Week 3-6 NAO predictive skill is attributed to stratospheric polar vortex conditions and ocean lower boundary forcing
- Enhanced NAO skill following weak vortex events results primarily from stratospheric coupling to the troposphere
- Enhanced NAO skill following strong vortex events can be attributed partly to ENSO

**Key words:** NAO predictive skill, attribution, stratosphere, ENSO

## **Abstract**

The week 3-6 averaged winter North Atlantic Oscillation (NAO) predictive skill in a state-of-the-art coupled climate prediction system is attributed to two principle sources: upper and lower boundary conditions linked to the stratosphere and El Niño-Southern Oscillation (ENSO), respectively. A 20-member ensemble of 45-day reforecasts over 1999-2015 is utilized, together with uninitialized simulations with the atmospheric component of the prediction system forced with observed radiative forcing and lower boundary conditions. NAO forecast skill for lead times out to six weeks is higher following extreme stratospheric polar vortex conditions (weak and strong vortex events) compared to neutral states. Enhanced week 3-6 NAO predictive skill for weak vortex events results primarily from stratospheric downward coupling to the troposphere, while enhanced skill for strong vortex events can be partly attributed to lower boundary forcing related to the ENSO phenomenon. Implications for forecast system development and improvement are discussed.

## **Plain Language**

Winter climate over Europe and eastern North America is significantly affected by variability of the North Atlantic Oscillation (NAO). In this study, we quantify the NAO predictive skill for lead times of 3-6 weeks and attribute it to two main sources: the stratosphere and the El Niño-Southern Oscillation (ENSO) phenomenon. This is done by contrasting ensembles of 45-day reforecasts over 1999-2015 with the corresponding uninitialized atmosphere model simulations forced with observed radiative forcing, sea-surface temperature and sea ice conditions. We find that the model is able to better predict the NAO up to six weeks following extreme weak or strong states of the stratospheric polar vortex compared to stratospheric neutral vortex states. Enhanced week 3-6 NAO predictive skill for weak vortex events results primarily from stratospheric coupling to the troposphere, while enhanced skill for strong vortex events can be attributed in part to lower boundary forcing related to ENSO. These results have implications for forecast model development and improvement.

## 1. Introduction

Forecasting of North Atlantic Oscillation (NAO) variability on subseasonal-to-seasonal (S2S) and seasonal-to-decadal (S2D) timescales has recently received much attention due to its potential to provide enormous social-economic benefits (White et al. 2017; Smith et al. 2019; Merryfield et al. 2020; Mariotti et al. 2020; Meehl et al. 2020). Winter climate over Europe and eastern North America is significantly affected by the variability of the NAO (Hurrell, 1995; 1996; Hurrell and Deser 2009). The temporal evolution of the NAO has been suggested to be primarily a stochastic process with a fundamental timescale of  $\sim 10$  days (Feldstein 2000) implying limited predictability beyond weather time scales (e.g., Johansson 2007). Yet, at longer timescales, a fraction of NAO variability has been shown to be forced by changes in sea-surface temperature (SST) and sea ice (e.g., Hurrell et al. 2004; Hoerling et al. 2004; Screen 2017). These low frequency NAO variations, therefore, are likely more than just statistical remnants of energetic high-frequency atmospheric fluctuations and could be predictable if they are driven by predictable changes in boundary forcing.

Recent forecast system assessments have suggested that there may be enhanced predictability of the NAO on S2S timescales (Riddle et al. 2013; Scaife et al. 2014). Efforts have been made to understand the source of this enhanced predictability (e.g., Cassou 2008; Newman and Sardeshmukh, 2008; Scaife et al., 2014; Brunet et al. 2015). Evidence suggests that stratospheric processes and associated variability are important (Tripathi et al., 2015a; Scaife et al., 2016; Wang et al. 2017; Jia et al. 2017; O'Reilly et al. 2018; Xiang et al. 2019; Nie et al. 2019), including the contribution of the stratospheric pathway associated with the El Niño-Southern Oscillation (ENSO) phenomenon (Domeisen et al., 2015; Butler et al., 2016; Domeisen et al. 2018).

Extreme stratospheric polar vortex states (i.e., weak and strong vortex events) are followed by anomalous near-surface NAO conditions (Baldwin and Dunkerton, 2001) implying enhanced

NAO prediction skill could occur as forecasts-of-opportunity contingent on initial stratospheric states (Albers and Newman 2019). For instance, Sigmond et al. (2013) demonstrated that the skill of NAO forecasts averaged over 15-60-day periods is substantially enhanced when forecasts are initialized at the onset time of weak stratospheric polar vortex events. Tripathi et al. (2015b) found that initialization based on anomalous vortex events improves the skill of NAO predictions up to week 4, which has also been supported by multiple S2S model assessments (WWRP/WCRP, 2018; Domeisen et al. 2020a, 2020b).

In these aforementioned studies, the role of the stratosphere is typically assessed by categorizing the individual forecasts based on initial stratospheric polar vortex states. However, this method cannot rule out the possibility that enhanced NAO predictive skill may also partly come from other sources, for instance lower-boundary forcing. Separating different sources of predictability is difficult, especially when the sample size is small. Surface boundary-forced NAO predictability can be inferred from uninitialized Atmosphere Model Intercomparison Project (AMIP) simulations prescribed with observed SST and sea ice conditions. By comparing the skill in a climate prediction system with its corresponding AMIP simulations, the relative importance of atmospheric (e.g., extreme stratospheric vortex states) and lower boundary sources of NAO predictability can be identified.

In this study we attribute boreal winter NAO predictive skill for lead times of 3-6 weeks to distinct physical sources. Reforecasts using a coupled model are analyzed to quantify skill dependency on the initial stratospheric conditions. Parallel uninitialized simulations employing the same modeling system are analyzed to isolate and quantify boundary forced predictability.

## **2. Model reforecasts and AMIP simulations**

95 *a. Model reforecast*

96       The reforecasts are conducted with the Community Earth System Model Version 1 (CESM;  
97 Hurrell et al. 2013) for 1999-2015. The daily output follows the protocol of the Subseasonal  
98 Experiment project (SubX; Pegion et al., 2019). The forecasts start every Wednesday and run for  
99 45 days. The atmospheric initial conditions are based on ERA-Interim reanalysis (Dee et al., 2002).  
100 The ocean and sea ice initial conditions come from a forced ocean-sea-ice simulation that employs  
101 adjusted Japanese 55-year Reanalysis atmospheric state fields and fluxes (Tsujino et al., 2018) as  
102 surface boundary conditions.

103       The CESM reforecast ensembles are generated using the random field initialization method  
104 (Magnusson et al., 2009). There are two 10-member ensembles with the same initial conditions  
105 but 30 (default) and 46 vertical levels in its atmospheric component – Community Atmosphere  
106 Model version 5 (CAM5; Neale et al., 2012; Richter et al., 2015). Richter et al., (2020) compared  
107 these two CESM reforecasts and found that improved representation of the stratosphere can  
108 improve the predictive skill of the stratosphere, but does not improve the NAO predictive skill.  
109 Therefore, we combine the two 10-member ensembles to yield a 20-member ensemble for detailed  
110 analysis. Our conclusions hold when we analyze the 10-member ensembles separately.

111       In addition, hindcasts with the National Centers for Environmental Prediction (NCEP)  
112 coupled forecast system model version 2 (CFS; Saha et al., 2014) and European Centre for  
113 Medium-Range Weather Forecasts (ECMWF; Vitart, 2014) are compared to those using CESM.  
114 This includes a 4-member CFS reforecast ensemble conducted every day for 1999-2010 and a 11-  
115 member ECMWF reforecast ensemble conducted twice per week for 1996-2015, both from the  
116 international S2S database (Vitart et al., 2016; 2017). Recognizing that the models have somewhat

different hindcast periods, all the findings presented here have been re-calculated using their common period of 1999-2010 and the results were not materially different.

#### *b. NAO skill evaluation*

We use the bias correction method used in SubX, where the daily anomaly for each variable is obtained by removing the daily climatology at different time lags (Pegion et al., 2019). The predictive skill is evaluated by the anomaly correlation coefficient (ACC) that has been commonly used in S2S forecasts (e.g., Tripathi et al., 2015b). Namely,

$$ACC = \frac{\sum x'_{model} x'_{obs}}{\sqrt{\sum (x'^2_{model} \sum x'^2_{obs})}}$$

where  $x'_{model}$  and  $x'_{obs}$  represent the weekly or monthly anomaly for models and observations (ERA-Interim reanalysis; Dee et al., 2002), respectively. We also calculate the root-mean-square error (RMSE) skill score between the model and observations (Wilks, 1995) and find smaller values but with roughly the same pattern as ACC (not shown).

In this study, we diagnose the NAO forecast skill of sea-level pressure (SLP) based on initialization during November-March for lead times of 3-6-weeks (day 15-42 average). Discrete weekly skill for lead times of 1- 6-weeks is also diagnosed. Similar to other studies (e.g., Johansson, 2007; Butler et al., 2016) we conduct Empirical Orthogonal Function (EOF) analysis for ERA-Interim monthly (November-March) SLP anomalies over the Atlantic sector (20°N-80°N; 90°W-40°E) and treat the leading EOF regression as the NAO pattern for both observations and models. The NAO index is then calculated by projecting the daily SLP anomaly from model and reanalysis data onto the leading EOF pattern and using it for ACC diagnostics. To quantify the confidence interval in the predictive skill of the NAO, we apply a bootstrapping method by resampling 10000 times with replacement and obtaining the 5% and 95% of the ACC significance levels (Mudelsee 2010).



The role of initial persistence in NAO predictability is evaluated by the correlation of the NAO anomaly relative to its week 0 value (day -3 to day 3 average), and the resulting monthly persistence skill is compared to that from the initialized dynamical models. Also, to isolate the role of surface lower boundary forcing, we utilize 50-member free-running atmosphere model simulations with CAM5 forced by observed greenhouse gases, SST and sea ice conditions (Hurrell et al., 2008). The ensemble-mean anomaly for the uninitialized AMIP forecast is obtained by removing the daily long-term climatology and then calculating the ACC against observations. Again, the analysis is of monthly mean variability, and the simulation skill is compared to the week 3-6 skill from initialized forecasts and from simple persistence.

To explore the role of the stratosphere in surface NAO predictability, we subsample the winter forecast into three categories based on the initial stratospheric zonal-mean zonal winds at 10 hPa and 60°N. Similar to Tripathi et al., (2015b), we first calculate the probability density function (PDF) of the 1999-2015 10-hPa 60°N November-March zonal-mean zonal wind distribution. The weak (strong) stratospheric polar vortex events can be defined for forecasts whose initial zonal wind at 10-hPa 60°N is below 10% of the PDF (3.55 m/s) or above 80% of the PDF (40.79 m/s). Note that slightly different thresholds are used so that the number of extreme events (60 weak and 62 strong vortex events) are comparable, but the results are not sensitive to the exact choice of thresholds. Figure S1 shows the composite of standardized polar-cap geopotential height and SLP anomalies for weak and strong vortex events, indicating that the observed downward coupling of extreme polar vortex events and their surface NAO features are both well captured in CESM. Neutral vortex events are defined for forecasts whose initial zonal wind at 10-hPa 60°N is between 30% and 70% of the PDF (17.18 m/s – 35.74 m/s; 154 cases). The predictive skills of persistence

and uninitialized AMIP simulations can be evaluated based on the same stratospheric events as in the CESM reforecasts.

### **3. Results**

#### *3.1. Winter NAO predictive skill*

The Northern Hemisphere (NH) monthly SLP hindcast skill from week 3 to 6 in boreal winter (November-March) for CESM (1999-2015), CFS (1999-2010) and ECMWF (1996-2015) models is presented in Figure 1a. The common feature among the three reforecasts is overall greater skill in lower-latitudes than higher-latitudes, with a secondary skill maximum centered over Greenland especially in CESM and ECMWF forecasts. When averaged over NH extratropics, ECMWF has the highest skill (0.36), followed by CESM (0.33) and CFS (0.26). In the Atlantic basin, high skill regions over Greenland and near the Azores project onto the NAO centers-of-action, suggesting that this leading mode of climate variability has particularly enhanced forecast skill (Johansson, 2007). CESM and ECMWF monthly SLP skill implies greater NAO predictability than indicated by CFS, a contrast among these systems that is evident already by week 2 and persists until week 6 (see Supplemental Figure S2).

Some of the model differences in skill are a function of ensemble size rather than a fundamental model bias that might plague a particular prediction system, and it has been shown that skill declines with diminishing model ensemble size (e.g., Kumar and Hoerling 1995; Butler et al. 2016; Athanasiadis et al. 2020; Smith et al. 2020). To explore this further, we randomly select  $N$  ensembles ( $N$  from 1 to 20) from the CESM reforecast and then conduct 1000-times bootstrapping to calculate the 5% and 95% statistical significance level of the NAO skill. Figure 1b shows the week 3-6 monthly NAO skill in CESM as a function of ensemble size. In agreement

with those earlier studies, the NAO skill approximately doubles (0.27 versus 0.51) when the ensemble size increases from 1 to 20, but it is close to saturation at 15 ensemble members (e.g., there is a less than 0.01 increase from 15 to 20 members).

Thus, when accounting for the differences in ensemble size of the systems diagnosed herein, the lower NAO skill in the smaller CFS ensemble is reconcilable with sampling alone; its skill overlaps with that of CESM when the latter's ensemble is sub-sampled to match the CFS population. That said, the lower skill with the CFS model might also be related to the fact that the stratospheric polar vortex is poorly predicted and stratosphere-troposphere coupling is too weak (Miller and Wang 2019). Evidence to support this argument for degraded skill is presented in the next section where we demonstrate an appreciable sensitivity of skill to stratospheric conditions overall.

As a prelude to a more detailed analysis of the attributable causes (sources) for week 3-6 NAO prediction skill, the initialized prediction skill of CESM is compared to that resulting from simple persistence, and that arising from lower boundary forcing alone with no recourse to the initial weather state. Summarized in Supplemental Figure S3, the monthly NAO skill in CESM hindcasts ( $\sim 0.5$ ) is found to be considerably larger than in both persistence forecasts ( $\sim 0.3$ ) and the simulation skill arising solely from effects of prescribed surface lower-boundary forcing ( $\sim 0.05$ ). It is interesting to note from their NH distributions of SLP skill (Supplemental Fig. S3, left) that the AMIP simulations have more than double the correlation skill of persistence averaged over the NH overall. But persistence skill is quite high over the two NAO centers of variability in the Atlantic basin, while AMIP skill is virtually absent over the NAO's northern node. This overall estimate of skill sources, while informative, obscures a considerable conditionality of the skill by each source.

### 3.2. Sensitivity to the stratospheric initial states

To explore the role of initial stratospheric states on NAO prediction skill, we subsample the CESM winter reforecasts into weak (60), neutral (154) and strong (62) polar vortex events. Figure 2a shows the monthly time series of 10 hPa zonal winds averaged along 60°N, the extreme values of which are used to identify strong (blue dots) and weak (red dots) vortex events during 1999-2015. The weekly NAO skill using this stratification is displayed in Figure 2b. In agreement with earlier studies, the NAO skill is generally higher in weeks 3–6 when initialized from extreme stratospheric polar vortex conditions compared to neutral states. Especially striking is the sustained high skill emerging from initial weak polar vortex conditions, having correlations above 0.5 through week 6. By week 6, the skill improvement relative to neutral states (0.23) is appreciable and statistically significant, indicating that NAO skill is substantially enhanced when initialized during weak vortex events, a result based on CESM that affirms prior findings based on other forecast systems (Sigmond et al. 2013; Tripathi et al. 2015; Domeisen et al. 2020b).

The results indicate that NAO skill when forecasts begin from strong and weak vortex events is comparable - and is moderately elevated compared to neutral vortex states during weeks 3 and 4. However, the skill decreases quickly in weeks 5 and 6 for strong vortex initializations, so that the improvement relative to neutral states becomes marginal (Figure 2b). This skill progression can be explained by a difference between CESM and observed NAO life cycles during strong vortex events. In weeks 5-6 following strong vortex events, the canonical positive NAO pattern is evident in CESM but not in observations (see Supplemental Figure S1b). We speculate that the lack of positive NAO skill in weeks 5-6 for these strong vortex cases might simply be due to

sampling rather than due to a fundamentally shorter time scale of stratosphere-troposphere interactions during strong versus weak vortex environments (c.f., figure 2 of Reichler et al. 2013).

The CESM SLP and NAO skill averaged for forecast lead times of 3-6 weeks under weak, neutral and strong polar vortex events is presented in Figure 3, and further elucidates the sensitivity to the stratospheric initial conditions. The higher NAO skill for weak vortex cases originates from a superior forecast performance over the northern center of NAO variability. There the monthly SLP correlation skill is near 0.7 for weak vortex conditions compared to slightly below 0.5 for the strong vortex cases. Interestingly, the NH average SLP skill is higher for the strong vortex environments (0.41 versus 0.34) and tends to also be higher in most locations, though with the clear regional exception being over the far North Atlantic.

The NAO skill for persistence forecasts and AMIP simulations provides further insight on the attributable causes for NAO prediction skill beyond two weeks (Figure 3b). The high skill for weak polar vortex initial states is not an outcome of particularly high persistence of the NAO during such states. Rather, NAO persistence skill following weak vortex initial conditions is significantly lower than for strong vortex states. There is also statistically significant asymmetry in AMIP simulation skill when binned according to reforecast polar vortex intensity. It is important to note that the AMIP runs are constrained only by variability in surface boundary conditions, and have no explicit synchronicity with the actual temporal variability of the polar vortex. Yet, the results of Fig. 3a can only be understood if those boundary forcings themselves force the NAO variability for the strong events.

Considering these two factors in aggregate reveals an absence of skill during weak vortex states in both persistence and AMIP, and that the considerable monthly skill of CESM predictions is mostly due to the importance of the initial stratospheric state. Note that the absence of

persistence skill implies a fundamentally nonlinear dynamical evolution in the forecasts that cannot be represented via simple persistence methods alone. By contrast, both persistence and lower boundary forcing contribute to monthly NAO skill when the initial polar vortex is strong.

An explanation for the role of ocean forcing is provided by an analysis that stratifies the occurrences of polar vortex events according to ENSO phase. The Niño 3.4 index in relation to weak and strong polar vortex events is shown in Fig. 4a. The relationship is not linear and is complicated. For instance, many strong vortex events appear to happen in either El Niño or La Niña years (e.g., 1999/2000, 2007/2008, 2009/2010, 2010/2011, 2015/2016), though this is less evident for weak and neutral events. This is evident from the histograms of Niño3.4 SST states stratified according to polar vortex intensity (Fig. 4b). The spread of the distribution for strong vortex states is wide and highly non-Gaussian (blue curve), especially compared to that for weak polar vortex states (red curve). It suggests that the NAO predictive skill following strong vortex events is influenced by ENSO, agreeing with the recent findings of Xiang et al. (2019) who identified ENSO as the most predictable subseasonal mode and found that its influence in the North Atlantic resembles the NAO pattern. However, further research is needed to determine why many strong vortex events coincide with both El Niño and La Niña years.

The lower panel of Fig. 4 provides a spatial view of the monthly SLP skill patterns related to effects of initial stratospheric upper air conditions and ENSO lower boundary conditions. Here we subsample the winter cases into extreme stratospheric polar vortex conditions (both weak and strong), ENSO cases (both El Niño and La Niña, defined by Niño3.4 index above/below  $\pm 0.5$ , respectively), and neutral stratosphere-ENSO cases (Figure 4b). Note that the ENSO cases have been excluded from the composites of extreme stratospheric vortex states, and extreme polar vortex events have been excluded from the ENSO cases. Immediately apparent is that SLP skill

for neutral stratosphere and neutral ENSO cases is negligibly low (Figure 4b middle panel), and has little amplitude in the NAO regional centers of variability. By contrast, SLP skill is comparatively high for extreme states of ENSO and the polar vortex. While the initial atmospheric state is an especially effective skill source over the northern node of the NAO, it is also clear that ENSO likewise projects onto centers of skill that align with the NAO dipole. These results demonstrate that both extreme stratospheric polar vortex states and extreme lower boundary forcing linked to ENSO account for week 3-6 NAO predictive skill during boreal winter.

#### 4. Summary and Discussion

In this study, we explore sources of subseasonal predictive skill of the boreal winter NAO. By utilizing ensembles of 45-day reforecasts during 1999-2015 with a state-of-the-art prediction system, in combination with uninitialized AMIP simulations, we attribute NAO predictive skill for lead times of 3-6 weeks. We find two principle sources of skill: upper and lower boundary constraints linked to the stratosphere and ENSO, respectively.

Specifically, we find that the winter NAO skill for forecast lead times out to six weeks is higher following extreme stratospheric polar vortex conditions (weak and strong vortex events) compared to neutral states. We further show that the enhanced NAO predictive skill for weak vortex events results primarily from stratospheric downward coupling, while the enhanced skill for strong vortex events can be attributed, in part, to lower boundary forcing associated with ENSO.

We also find that NAO prediction skill can be significantly reduced if the forecast ensemble size is too small. While a similar result has been determined for seasonal and decadal prediction systems, it may become more important for the subseasonal forecast due to compromise between ensemble size and running frequency. Our finding suggests that given fixed computational

resources, the ensemble size should be no less than 10; otherwise, NAO predictive skill will be substantially lower than achievable levels.

Our findings come with a caveat that CESM and most other similar subseasonal forecast systems (e.g., S2S Prediction Project and SubX) cover only the most recent 20-30 years. Since NAO predictability has been found to vary at decadal and multidecadal timescale (Weisheimer et al. 2018), the degree to which our results are specific to the period analyzed is still an open question.

Our findings also have important implications for forecast system development and improvement. Specifically, our results indicate that NAO boreal winter forecast skill depends on not only the representation of stratospheric processes in the forecast model, but also on the ENSO evolution during the model testing period. Thus, for NAO predictive skill as benchmark for model improvement, the analysis of subseasonal reforecasts in combination with AMIP simulations will provide insight as to whether NAO predictive skill can be improved by focusing on better representation of stratospheric processes and related variability in a specific prediction system, or through better simulation of ENSO, if not both.

## **Acknowledgements**

This study was funded by NOAA's Climate Program Office (CPO) Modeling, Analysis, Predictions and Projections (MAPP). This work was supported by the National Center for Atmospheric Research, which is a major facility sponsored by the National Science Foundation under Cooperative Agreement No. 1852977. Portions of this study were supported by the Regional and Global Model Analysis (RGMA) component of the Earth and Environmental System Modeling Program of the U.S. Department of Energy's Office of Biological & Environmental Research (BER) via National Science Foundation IA 1844590. We thank Yan Wang at NOAA's



322 Physical Sciences Laboratory for her help with downloading CFS and ECMWF hindcast data and  
323 Dr. Zac Lawrence for helpful comments on an earlier version of this paper. The CESM reforecast  
324 data is available to the public via Columbia University's International Research Institute for  
325 Climate and Society (IRI) library at  
326 <http://iridl.ldeo.columbia.edu/SOURCES/.Models/.SubX/.CESM/>. The CAM5 simulations are  
327 available at PSL's Facility for Weather and Climate Assessments (FACTS) website at  
328 <https://www.esrl.noaa.gov/psl/repository/facts/>. The CFS and ECMWF data is available at  
329 ECMWF's S2S portal <https://apps.ecmwf.int/datasets/data/s2s/levtype=sfc/origin=ecmf/type=cf/>.

## 330    **Reference**

- 331    Albers, J. R., & Newman, M. (2019). A priori identification of skillful extratropical subseasonal  
332    forecasts. *Geophysical Research Letters*, 46, 12,527–12,536. [https://doi.org/10.1029/](https://doi.org/10.1029/2019GL085270)  
333    2019GL085270
- 334    Athanasiadis, P.J., Yeager, S., Kwon, Y. et al. (2020): Decadal predictability of North Atlantic  
335    blocking and the NAO. *npj Clim Atmos Sci*, 3, 20. <https://doi.org/10.1038/s41612-020-0120-6>.
- 336    Baldwin, M. P., and T. J. Dunkerton, 2001: Stratospheric harbingers of anomalous weather  
337    regimes. *Science*, 294, 581–584, <https://doi.org/10.1126/science.1063315>.
- 338    Brunet, G., S. Jones, and P. M. Ruti, Eds., (2015): Seamless prediction of the Earth system: From  
339    minutes to months. WMO-1156, 483 pp., [https://library.wmo.int/pmb\\_ged/wmo\\_1156\\_en.pdf](https://library.wmo.int/pmb_ged/wmo_1156_en.pdf).
- 340    Butler, A. H., Arribas, A., Athanassiadou, M., Baehr, J., Calvo, N., Charlton-Perez, and co-authors  
341    (2016): The Climate-system Historical Forecast Project: do stratosphere-resolving models make  
342    better seasonal climate predictions in boreal winter? *Q.J.R. Meteorol. Soc.*, 142, 1413–1427.  
343    <https://doi.org/10.1002/qj.2743>
- 344    Butler, A. H., and L. M. Polvani, (2011): El Niño, La Niña, and strato- spheric sudden warmings:  
345    A reevaluation in light of the obser- vational record. *Geophys. Res. Lett.*, 38, L13807, doi:10.1029/  
346    2011GL048084.
- 347    Butler, A. H., L. M. Polvani and C. Deser, (2014): Separating the stratospheric and tropospheric  
348    pathways of El Niño–Southern Oscillation teleconnections. *Environ. Res. Lett.*, 9, 024014,  
349    doi:10.1088/ 1748-9326/9/2/024014.
- 350    Cassou, C., (2008): Intraseasonal interaction between the Madden–Julian Oscillation and the North  
351    Atlantic Oscillation. *Nature*, 455, 523–527, doi:10.1038/nature07286.
- 352    Dee, D. P., Uppala, S. M., Simmons, A. J., Berrisford, P., Poli, P., Kobayashi, S., ....Vitart, F.  
353    (2011). The ERA-Interim reanalysis: Configuration and performance of the data assimilation  
354    system, *Quart. J. Roy. Meteor. Soc.*, 137, 553–597, <https://doi.org/10.1002/qj.828>
- 355    Dennis, J., Edwards, J., Evans, K., Guba, O., Lauritzen, P., Mirin, A., ... Worley P. (2012). CAM-  
356    SE: A scalable spectral element dynamical core for the Community Atmosphere Model, *Int. J.*  
357    *High Perform. Comput. Appl.*, 26(1), 74–89. <https://doi.org/10.1177/1094342011428142>.
- 358    Domeisen, D. I. V., A. H. Butler, K. Fröhlich, M. Bittner, W. Müller, and J. Baehr, (2015):  
359    Seasonal predictability over Europe arising from El Niño and stratospheric variability in the MPI-  
360    ESM seasonal prediction system. *J. Climate*, 28, 256–271, [https://doi.org/10.1175/JCLI-D-14-](https://doi.org/10.1175/JCLI-D-14-00207.1)  
361    00207.1.
- 362    Domeisen, D. I. V., Butler, A. H., Charlton-Perez, A. J., Ayarzagüena, B., Baldwin, M. P., Dunn-  
363    Sigouin, E., et al (2020a). The role of the stratosphere in subseasonal to seasonal prediction: 1.

364 Predictability of the stratosphere. *Journal of Geophysical Research: Atmospheres*, 125,  
365 e2019JD030920. <https://doi.org/10.1029/2019JD030920>

366 Domeisen, D. I., Butler, A. H., Charlton-Perez, A. J., Ayarzagüena, B., Baldwin, M. P., Dunn-  
367 Sigouin, E. et al. (2020b). The role of the stratosphere in subseasonal to seasonal prediction: 2.  
368 Predictability arising from stratosphere-troposphere coupling. *Journal of Geophysical Research:*  
369 *Atmospheres*, 125, e2019JD030923. <https://doi.org/10.1029/2019JD030923>.

370 Domeisen, D. I. V., C. I. Garfinkel, and A. H. Butler, (2018): The teleconnection of El Niño  
371 Southern Oscillation to the stratosphere. *Rev. Geophys.*, 57, 5–47,  
372 <https://doi.org/10.1029/2018RG000596>.

373 Feldstein, S.B., (2000): Teleconnections and ENSO, the timescale, power spectra, and climate  
374 noise properties. *J. Climate* 13, 4430–4440. [https://doi.org/10.1175/1520-  
375 \*0442\(2000\)013%3C4430:TTPSAC%3E2.0.CO;2\*.](https://doi.org/10.1175/1520-0442(2000)013%3C4430:TTPSAC%3E2.0.CO;2)

376 Hoerling, M. P., J. W. Hurrell, T. Xu, G. T. Bates, and A. S. Phillips, (2004): Twentieth century  
377 North Atlantic climate change. Part II: Understanding the effect of Indian Ocean warming. *Clim.*  
378 *Dyn.*, 23, 391–405, doi:10.1007/s00382-004-0433-x.

379 Hurrell, J. W., (1995): Decadal trends in the North Atlantic Oscillation: Regional temperatures and  
380 precipitation. *Science*, 269, 676–679. DOI: 10.1126/science.269.5224.676.

381 Hurrell, J. W., (1996): Influence of variations in extratropical wintertime teleconnections on  
382 Northern Hemisphere temperature. *Geophys. Res. Lett.*, 23, 665–668,  
383 <https://doi.org/10.1029/96GL00459>.

384 Hurrell, J. W., and C. Deser, (2009): North Atlantic climate variability: The role of the North  
385 Atlantic Oscillation. *J. Mar. Syst.*, 78, 28–41, doi:10.1016/j.jmarsys.

386 Hurrell, J. W., Hack, J. J., Shea, D., Caron, J. M. & Rosinski, J. (2008). A new sea surface  
387 temperature and sea ice boundary dataset for the community atmosphere model. *J. Climate*, 21,  
388 5145–53. <https://doi.org/10.1175/2008JCLI2292.1>

389 Hurrell, J. W., M. P. Hoerling, A. S. Phillips, and T. Xu, (2004): Twentieth century north Atlantic  
390 climate change. Part I: assessing determinism. *Clim. Dyn.*, 23, 371–389, doi:10.1007/s00382-004-  
391 0432-y.

392 Jia, L., and Coauthors, (2017): Seasonal Prediction Skill of Northern Extratropical Surface  
393 Temperature Driven by the Stratosphere. *J. Climate*, 30, 4463–4475, [https://doi.org/10.1175/JCLI-  
394 \*D-16-0475.1\*.](https://doi.org/10.1175/JCLI-D-16-0475.1)

395 Jiménez-Esteve, B., and D. I. V. Domeisen, (2018): The Tropospheric Pathway of the ENSO–  
396 North Atlantic Teleconnection. *J. Climate*, 31, 4563–4584, [https://doi.org/10.1175/JCLI-D-17-](https://doi.org/10.1175/JCLI-D-17-0716.1)  
397 *0716.1*.

398 Johansson, Ake, (2007): Prediction skill of the NAO and PNA from daily to seasonal timescale,  
399 *Journal of Climate*, 20, 1957-1975, doi:10.1175/JCLI4072.1.

400 Kumar, A., and M. P. Hoerling, 1995: Prospects and limitation of seasonal atmospheric GCM  
401 predictions. *Bull. Amer. Meteor. Soc.*, 76, 335-345.

402 L’Heureux, M. L., Tippett, M. K., Kumar, A., Butler, A. H., Ciasto, L. M., Ding, Q., ... Johnson,  
403 N. C. (2017): Strong relations between ENSO and the Arctic Oscillation in the North American  
404 Multimodel Ensemble. *Geophysical Research Letters*, 44, 11,654–11,662.  
405 <https://doi.org/10.1002/2017GL074854>.

406 Magnusson, Linus, Jonas Nycander & Erland Källén (2009): Flow-dependent versus flow-  
407 independent initial perturbations for ensemble prediction, *Tellus A: Dynamic Meteorology and*  
408 *Oceanography*, 61:2, 194-209, DOI: 10.1111/j.1600-0870.2008.00385.x.

409 Mariotti, A., and Coauthors, (2020): Windows of Opportunity for Skillful Forecasts Subseasonal  
410 to Seasonal and Beyond. *Bull. Amer. Meteor. Soc.*, 101, E608–E625,  
411 <https://doi.org/10.1175/BAMS-D-18-0326.1>.

412 Meehl, G. A., and Coauthors, (2020): Initialized Earth system prediction from subseasonal to  
413 decadal timescales, *Nature Reviews Earth and Environment*, in review.

414 Merryfield, W. J., and Coauthors, (2020): Current and emerging developments in subseasonal to  
415 decadal prediction. *Bull. Amer. Meteor. Soc.*, doi: <https://doi.org/10.1175/BAMS-D-19-0037.1>.

416 Miller, D. E., and Z. Wang, (2019): Assessing Seasonal Predictability Sources and Windows of  
417 High Predictability in the Climate Forecast System, Version 2. *J. Climate*, 32, 1307–1326,  
418 <https://doi.org/10.1175/JCLI-D-18-0389.1>.

419 Mudelsee M (2010): Climate Time Series Analysis: Classical Statistical and Bootstrap Methods.  
420 First edition. Springer, Dordrecht, 474pp

421 Neale, R. B. and Coauthors (2012). Description of the NCAR community atmosphere model  
422 (CAM 5.0) NCAR, *Technical Note*, NCAR, TN 486.  
423 ([http://www.cesm.ucar.edu/models/cesm1.0/cam/docs/description/cam5\\_desc.pdf](http://www.cesm.ucar.edu/models/cesm1.0/cam/docs/description/cam5_desc.pdf)).

424 Newman, M., & Sardeshmukh, P. D. (2008): Tropical and stratospheric influences on extratropical  
425 short-term climate variability. *Journal of Climate*, 21, 4326.  
426 <https://doi.org/10.1175/2008JCLI2118.1>

427 Nie, Y., A. A. Scaife, H-L Ren, R. E Comer, M. B Andrews, P. Davis and N. Marin, (2019):  
428 Stratospheric initial conditions provide seasonal predictability of the North Atlantic and Arctic  
429 Oscillations. *Environ. Res. Lett.* 14 034006.

430 O'Reilly CH, Weisheimer A, Woollings T, Gray LJ, MacLeod D. (2019): The importance of  
 431 stratospheric initial conditions for winter North Atlantic Oscillation predictability and implications  
 432 for the signal-to-noise paradox. *Q J R Meteorol Soc.* 145:131–146. <https://doi.org/10.1002/qj.3413>.

433 Pegion, K., and Coauthors, (2019): The Subseasonal Experiment (SubX): A multi-model  
 434 subseasonal prediction experiment. *Bull. Amer. Meteor. Soc.*, 100, 2043–2060, <https://doi.org/10.1175/BAMS-D-18-0270.1>.

436 Polvani, L., Sun, L., Butler, A. H., Richter, J. H., & Deser, C. (2017). Distinguishing stratospheric  
 437 sudden warmings from ENSO as key drivers of wintertime climate variability over the North  
 438 Atlantic and Eurasia, *J. Climate*, 30(6), 1959–1969. <https://doi.org/10.1175/JCLI-D-16-0277.1>

439 Reichler, T., Kim, J., Manzini, E. et al. (2012): A stratospheric connection to Atlantic climate  
 440 variability. *Nature Geosci* 5, 783–787. <https://doi.org/10.1038/ngeo1586>

441 Richter, J. H., C. Deser, and L. Sun, (2015): Effects of stratospheric variability on El Niño  
 442 teleconnections. *Environ. Res. Lett.*, 10, 124021, doi:10.1088/1748-9326/10/12/124021.

443 Richter, J. H., K. Pegion, L. Sun, H. Kim, J. M. Caron, A. Glanville, S. Yeager, W. Kim and A.  
 444 Tawfik, (2020): Subseasonal prediction with CESM1 and the role of stratospheric variability on  
 445 subseasonal prediction skill, *Weather and Forecasting*, In review.

446 Riddle, E. E., Stoner, M. B., Johnson, N. C., L'Heureux, M. L., Collins, D. C., & Feldstein, S. B.  
 447 (2013): The impact of the MJO on clusters of wintertime circulation anomalies over the North  
 448 American region. *Climate Dynamics*, 40, 1749–1766. [https://doi.org/10.1007/s00382-012-1493-](https://doi.org/10.1007/s00382-012-1493-y)  
 449 [y](https://doi.org/10.1007/s00382-012-1493-y).

450 Saha, S., S. Moorthi, X. Wu, J. Wang, and Coauthors, (2014): The NCEP Climate Forecast System  
 451 Version 2. *Journal of Climate*, 27, 2185–2208, doi:10.1175/JCLI-D-12-00823.1.

452 Scaife, A. A., et al. (2014), Skillful long-range prediction of European and North American winters,  
 453 *Geophys. Res. Lett.*, 41, 2514–2519, doi:10.1002/2014GL059637.

454 Scaife, A. A., Karpechko, A. Y., Baldwin, M. P., Brookshaw, A., Butler, A. H., Eade, R., et al.  
 455 (2016). Seasonal winter forecasts and the stratosphere. *Atmospheric Science Letters*, 17(1), 51–  
 456 56., doi:10.1002/asl.598.

457 Screen, J. The missing Northern European winter cooling response to Arctic sea ice loss. *Nat*  
 458 *Commun* 8, 14603 (2017). <https://doi.org/10.1038/ncomms14603>.

459 Sigmond, M., J. Scinocca, V. Kharin, and T. Shepherd, (2013): Enhanced seasonal forecast skill  
 460 following stratospheric sudden warmings. *Nat. Geosci.*, 6, 98–102, doi:10.1038/ngeo1698.

461 Smith, D. M., and Coauthors, (2019): Robust skill of decadal climate predictions. *npj Clim. Atmos.*  
 462 *Sci.*, 2, 1–10, doi:10.1038/s41612-019-0071-y.

Smith, D.M., Scaife, A.A., Eade, R. et al. (2020): North Atlantic climate far more predictable than models imply. *Nature*, 583, 796–800. <https://doi.org/10.1038/s41586-020-2525-0>.

Tripathi, O. P., Baldwin, M., Charlton-Perez, A., Charron, M., Eckermann, S. D., Gerber, E., Harrison, R. G., Jackson, D. R., Kim, B.-M., Kuroda, Y., Lang, A., Mahmood, S., Mizuta, R., Roff, G., Sigmond, M. and Son, S.-W. (2015a) Review: the predictability of the extra-tropical stratosphere on monthly timescales and its impact on the skill of tropospheric forecasts. *Quarterly Journal of the Royal Meteorological Society*, 141 (689). pp. 987-1003. doi: 10.1002/qj.2432

Tripathi, O. P., Charlton-Perez, A., Sigmond, M. and Vitart, F. (2015b) Enhanced long-range forecast skill in boreal winter following stratospheric strong vortex conditions. *Environmental Research Letters*, 10 (10). 104007. doi: 10.1088/1748-9326/10/10/104007.

Tsujino, H., S. Urakawa, H. Nakano, R. J. Small, W. M. Kim, S. G. Yeager, et al., (2018): JRA-55 based surface dataset for driving ocean-sea-ice models. *Ocean Model.*, doi:10.1016/j.ocemod.2018.07.002.

Vitart, F. 2014: Evolution of ECMWF sub-seasonal forecast skill scores. *Quart. J. Roy. Meteor. Soc.*, 140, 1889-1899.

Vitart F and Coauthors 2016. The sub-seasonal to seasonal prediction (S2S) project database. *Bull. Am. Meteorol. Soc.* 98: 163–173. <https://doi.org/10.1175/BAMS-D-16-0017.1>.

Vitart, F. and Coauthors (2017). The Subseasonal to Seasonal (S2S) prediction project database. *Bulletin of the American Meteorological Society*, 98, 163–173. <https://doi.org/10.1175/BAMS-D-16-0017.1>

Vitart, F., Robertson, A. & Anderson, D. Sub-seasonal to Seasonal Prediction Project, 2012: bridging the gap between weather and climate. *WMO Bull.* 61, 23–28.

Wang, L., Ting, M., & Kushner, P. J. (2017): A robust empirical seasonal prediction of winter NAO and surface climate. *Scientific Reports*, 7(1), 279. <https://doi.org/10.1038/s41598-017-00353-y>.

Weisheimer, A., Decremmer, D., Macleod, D., O'Reilly, C., Stockdale, T. N., Johnson, S., & Palmer, T. N. (2018). How confident are predictability estimates of the winter North Atlantic Oscillation? *Quarterly Journal of the Royal Meteorological Society*, 145(S1), 140–159.

White, Christopher J. et al., (2017): Potential applications of subseasonal-to-seasonal (S2S) predictions, *Met. Apps*, 24: 315-325. doi:10.1002/met.1654.

Wilks, D. S. (1995), *Statistical Methods in the Atmospheric Sciences: An Introduction*, 467 pp., Academic, San Diego, Calif.

WWRP/WCRP, 2018: WWRP/WCRP Sub-seasonal to Seasonal Prediction Project (S2S) Phase II Proposal.

504  
505 Xiang, B., Lin, S.-J., Zhao, M., Johnson, N. C., Yang, X., & Jiang, X. (2019): Subseasonal week  
506 3–5 surface air temperature prediction during boreal wintertime in a GFDL model. *Geophysical*  
507 *Research Letters*, 46. <https://doi.org/10.1029/2018GL081314>.

## 508 List of Figures

509 **Figure 1:** (a) Sea-level pressure week 3-6 predictive skill evaluated by anomaly correlation  
510 coefficient (ACC) during November-March (NDJFM) for CESM, CFS and ECMWF reforecasts.  
511 Values on the left corner denote the skill averaged over Northern hemisphere extratropics.  
512 Numbers in the brackets of each model show the ensemble size. (b) Week 3-6 North Atlantic  
513 Oscillation (NAO) predictive skill as a function of ensemble size. Shading denotes the 5% and 95%  
514 statistical level of the CESM reforecast by conducting bootstrapping. Blue (red) error bars indicate  
515 the 5% and 95% statistical level of CFS and ECMWF reforecasts, respectively.

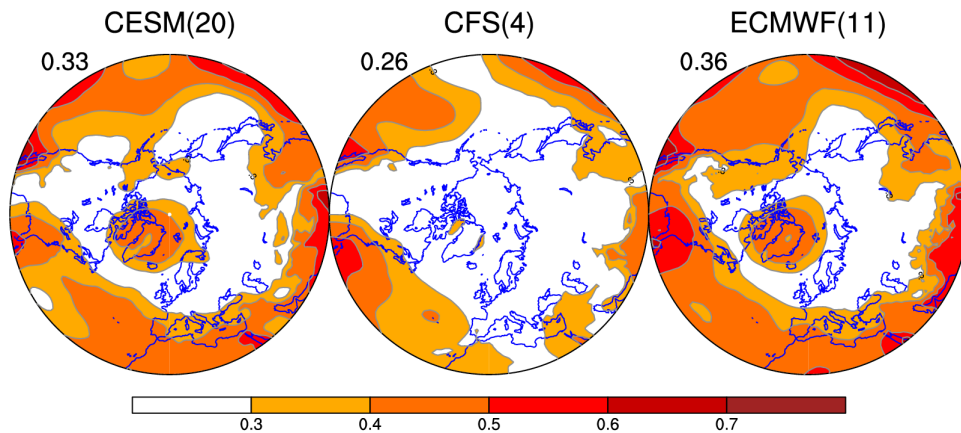
516  
517 **Figure 2:** (a) Observed Nov-March zonal-mean zonal wind at 10hPa and 60°N and the weak (red),  
518 strong (blue) polar vortex CESM reforecast cases. (b) Weekly NAO skill for the weak (red), strong  
519 (blue) stratospheric polar vortex events and neutral polar vortex conditions (gray). Error bars  
520 indicate the 5% and 95% statistical level based on 10000-time bootstrapping.

521  
522 **Figure 3:** (a) Sea-level pressure week 3-6 predictive skill for weak, neutral and strong polar vortex  
523 events. Values on the left corner denote the average of the ACC averaged over NH extratropics.  
524 (b) As in (a), but for the NAO skill in CESM, persistence and uninitialized AMIP simulations.  
525 Error bars indicate the 5% and 95% statistical levels by bootstrapping.

526  
527 **Figure 4:** (a) Niño3.4 time series and the weak (red dots) and strong (blue dots) polar vortex events  
528 and the probability density function of Niño3.4 index for the weak (red), neutral (gray shading)  
529 and strong (blue) polar vortex events. In (a) the daily Niño3.4 index is smoothed by 31 days  
530 running mean. (b) sea-level pressure predictive skill for initial extreme stratospheric polar vortex  
531 events (bottom left; combining weak and strong events), neutral stratosphere-ENSO events  
532 (bottom middle) and ENSO events. Values on the left corner denote the skill averaged over NH  
533 extratropics.



### a) SLP skill



### b) NAO skill

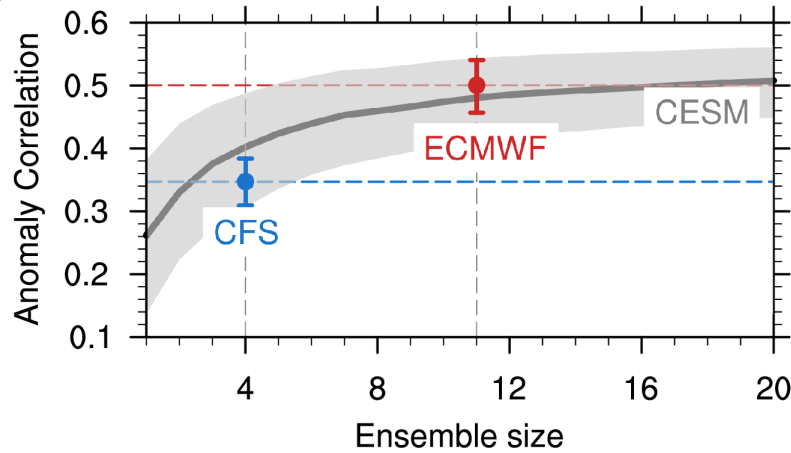


**Figure 1:** (a) Sea-level pressure week 3-6 predictive skill evaluated by anomaly correlation coefficient (ACC) during November-March (NDJFM) for CESM, CFS and ECMWF reforecasts. Values on the left corner denote the skill averaged over Northern hemisphere (NH) extratropics. Numbers in the brackets of each model show the ensemble size. (b) Week 3-6 North Atlantic Oscillation (NAO) predictive skill as a function of ensemble size. Shading denotes the 5% and 95% statistical level of the CESM reforecast by conducting bootstrapping. Blue (red) error bars indicate the 5% and 95% statistical level of CFS and ECMWF reforecasts, respectively.

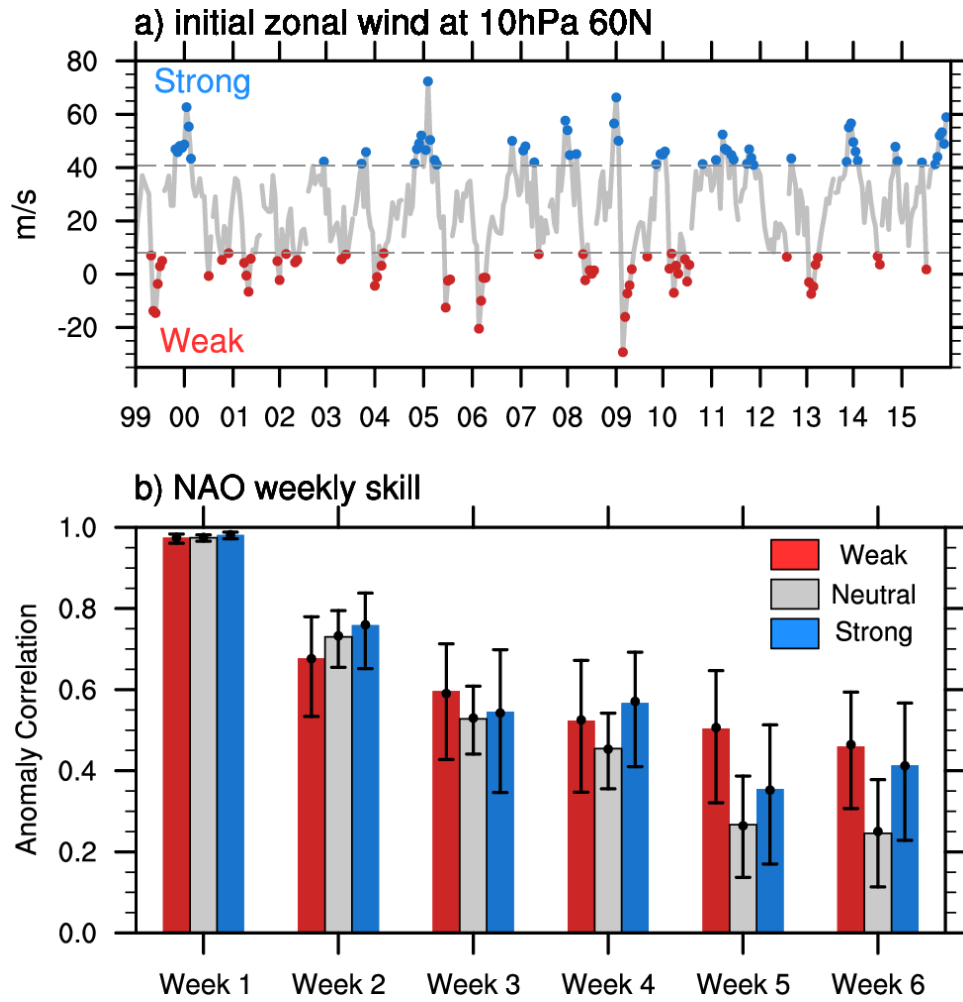


**Figure 2:** (a) Observed Nov-March zonal-mean zonal wind at 10hPa and 60°N and the weak (red), strong (blue) polar vortex CESM reforecast cases. (b) Weekly NAO skill for the weak (red), strong (blue) stratospheric polar vortex events and neutral polar vortex conditions (gray). Error bars indicate the 5% and 95% statistical level based on 1000-time bootstrapping.

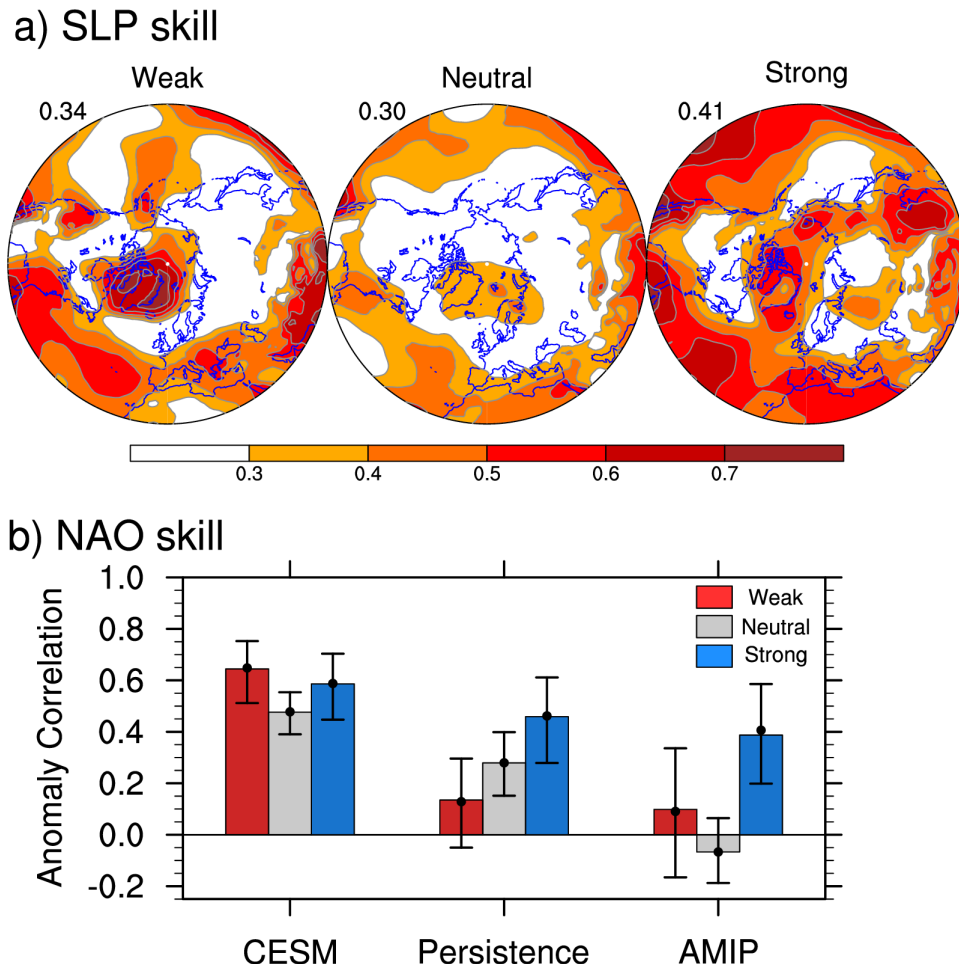


**Figure 3:** (a) Sea-level pressure week 3-6 predictive skill for weak, neutral and strong polar vortex events. Values on the left corner denote the average of the ACC averaged over NH extratropics. (b) As in (a), but for the NAO predictive skill in CESM, persistence and uninitialized AMIP simulations. Error bars indicate the 5% and 95% statistical levels by bootstrapping.

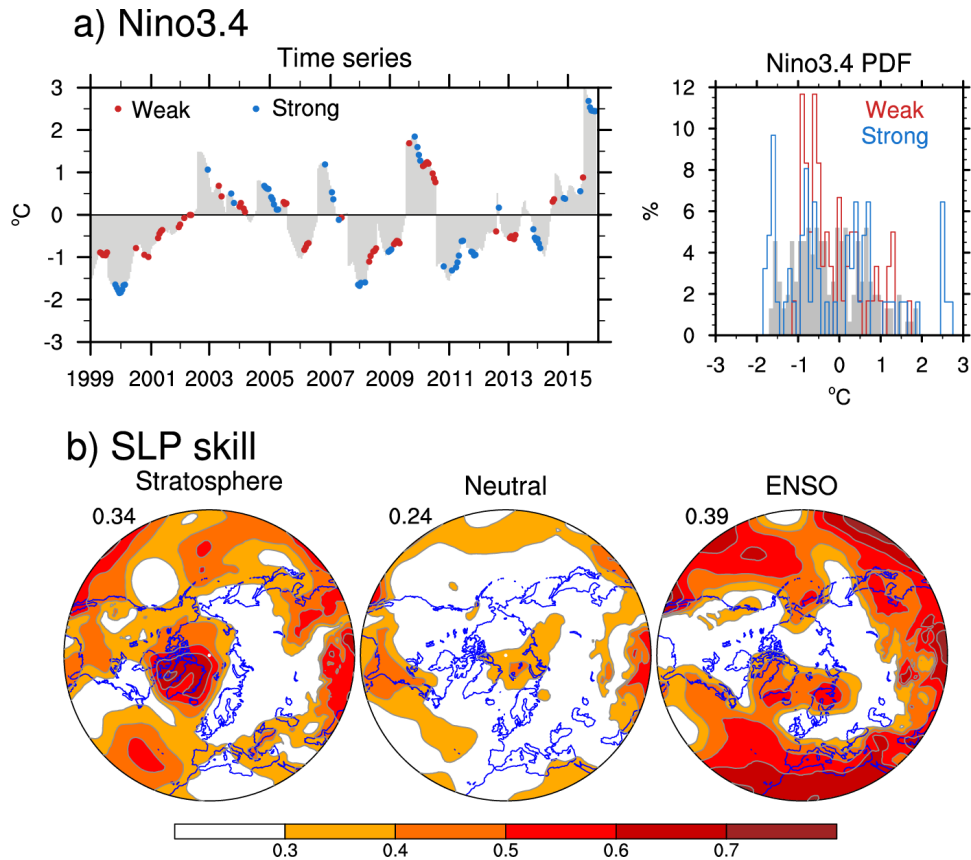


**Figure 4:** (a) Niño3.4 time series and the weak (red dots) and strong (blue dots) polar vortex events and the probability density function of Niño3.4 index for the weak (red), neutral (gray shading) and strong (blue) polar vortex events. In (a) the daily Niño3.4 index is smoothed by 31 days running mean. (b) sea-level pressure predictive skill for initial extreme stratospheric polar vortex events (bottom left; combining weak and strong events), neutral stratosphere-ENSO events (bottom middle) and ENSO events. Values on the left corner denote the skill averaged over NH extratropics.

**Supplementary Information for**  
**Attribution of NAO predictive skill beyond two weeks in boreal winter**

Lantao Sun<sup>1\*</sup>, Judith Perlwitz<sup>2</sup>, Jadwiga (Yaga) Richter<sup>3</sup>,

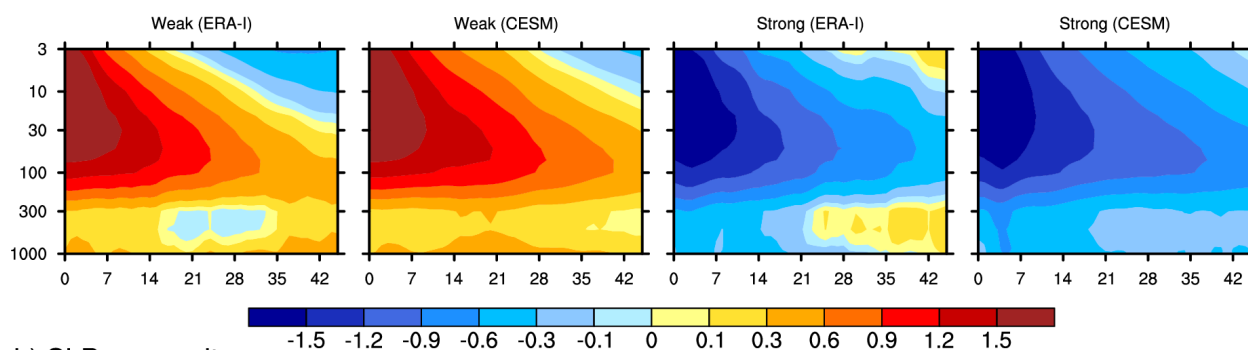
Martin Hoerling<sup>2</sup>, James W. Hurrell<sup>1</sup>

<sup>1</sup> Department of Atmospheric Science, Colorado State University, Fort Collins, CO

<sup>2</sup>NOAA Earth System Research Laboratory Physical Science Division, Boulder, CO

<sup>3</sup>National Center for Atmospheric Research, Boulder, CO

a) Polar-cap Z3 composite



b) SLP composite

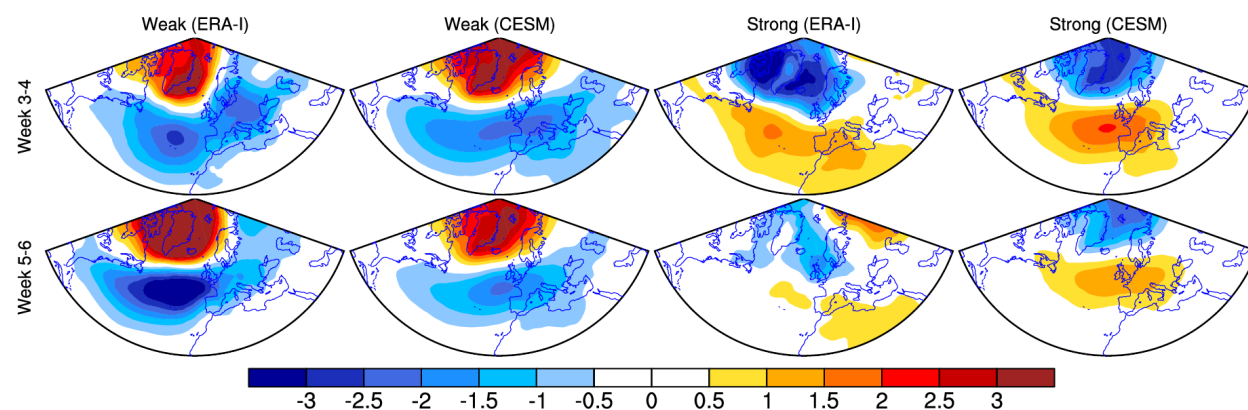


**Figure S1:** a) Composite of the standardized polar-cap geopotential height anomalies for weak and strong polar vortex events based on ERA-Interim and CESM reforecast. b) As in a), but for the anomalous sea-level pressure (SLP) composite based on ERA-Interim and week 3-4/5-6 of the CESM reforecast.

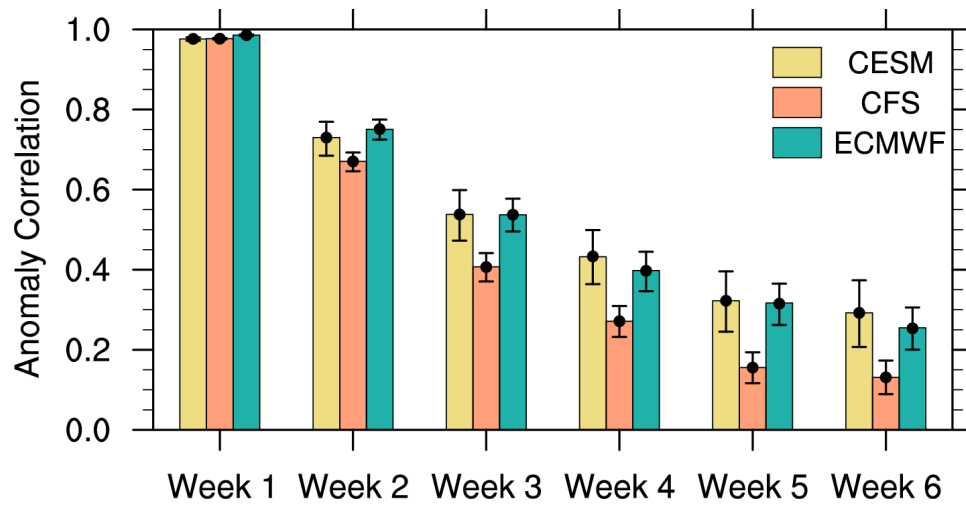
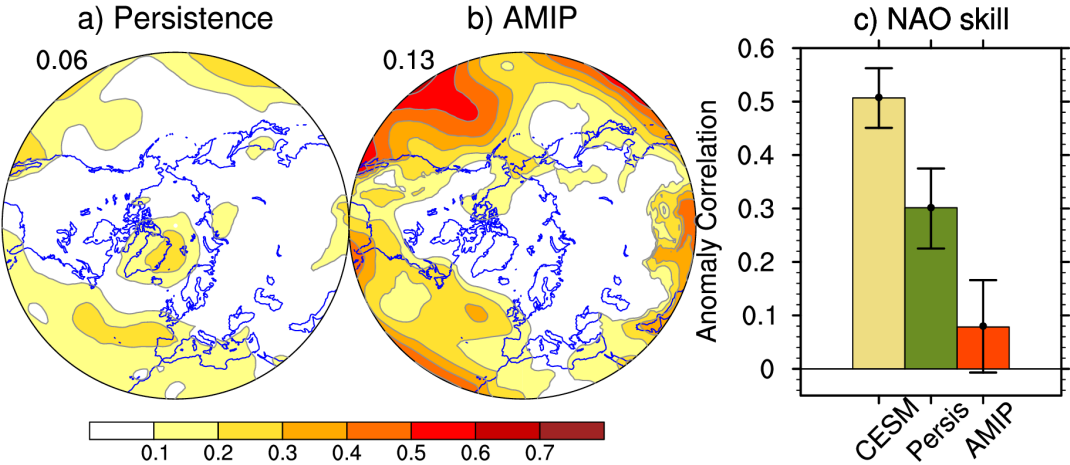


**Figure S2:** Weekly North Atlantic Oscillation (NAO) skill for CESM, NCEP and ECMWF. Error bars indicate the 5% and 95% statistical level based on 10000 bootstrap resamples.



25  
26

27 **Figure S3:** As in Fig. 1a, but for the SLP predictive skill due to persistence (a) and in the  
28 uninitialised AMIP simulations (b). Values on the left corner denote the skill averaged over  
29 northern hemisphere extratropics. c) week 3-6 NAO skill comparison among CESM, persistence  
30 and uninitialised AMIP simulations. Error bars indicate the 5% and 95% statistical levels by  
31 bootstrapping.